Revised analysis of negative capacitance in ferroelectric-insulator capacitors: analytical and numerical results, physical insight, comparison to experiments.

T. Rollo[1], F. Blanchini[2], G. Giordano[3], R. Specogna[1], D. Esseni[1]

[1]DPIA, University of Udine, Via delle Scienze 206, 33100 Udine, Italy; email: david.esseni@uniud.it; [2]DMIF, University of Udine, Via delle Scienze 206, 33100 Udine, Italy; [3]Delft Center for Systems and Control, Delft University of Technology, Delft, The Netherlands.

I. Abstract

We present a revised analysis of Negative Capacitance (NC) in ferroelectric-insulator capacitors, and particularly of the difference between systems *with* and *without* a metal interlayer. We develop a model accounting for the three-dimensional electrostatics and report analytical and numerical results based on Landau-Ginzburg equations. Our results explain the lack of NC operation in capacitors having an interlayer metal, compare well with recent experiments and enlighten the role of traps at the ferroelectric-oxide interface.

II. Introduction

Recent experiments on Metal-Ferroelectric-Insulator-Metal (MFIM) structures claimed a direct observation of NC operation [1], [2], but other contributions focused on Metal-Ferroelectric-Metal-Insulator-Metal (MFMIM) capacitors negated any evidence of NC operation [3], or proposed that the alleged NC effects are always due to domains switching [3]–[6]. From a theory perspective it was argued that domain nucleation is much more likely to occur in a MFMIM than in a MFIM system [7], but such conclusions relied on the inspection of energy landscapes of a one-dimensional system, rather than on actual dynamic equations. Hence NC stabilization of ferroelectrics is still actively debated [8].

We here present a study of the NC operation in MFIM and MFMIM systems. First we develop a model based on the Landau-Ginzburg (LG) theory that accounts for the three-dimensional electrostatics. Then we derive analytical conditions for a stable NC operation and provide physical insight by solving numerically the LG equations. Our results explain the lack of NC operation in MFMIM capacitors and compare well with experiments [1], [2]. We also show that traps at the ferroelectric-oxide interface may play an important role.

III. Dynamic equations for ferroelectric domains

By following [7], we write the free energy per unit volume of the ferroelectric as in **Eq.1**, where P is the spontaneous polarization, $\alpha<0$, β and γ are the ferroelectric anisotropy constants, E_F, ε_F are respectively the electric field and relative background permittivity of the ferroelectric, while k is the coupling constant governing the domain wall energy. When we consider the MFIM and MFMIM systems sketched in **Fig.1** the overall electrostatic energy consists of the three contributions defined as in **Eq.2** [9], namely the ferroelectric self-energy $\mathcal{U}_F$, the term $\mathcal{U}_B$ of the external battery, and the depolarization energy $\mathcal{U}_D$ (which is zero in a MFM structure). In **Eq.2** $E_{F,T}(\bar{r})=E_{F,z}(\bar{r},-t_F)$ is the electric field at the top metal interface and n_D is the number of domains. When we sum $\mathcal{U}_F$, $\mathcal{U}_B$, $\mathcal{U}_D$ and normalize to the domain area d^2 we obtain **Eq.3**. **Eq.4** reports the contribution, $u_{W,i}$, of domain i to the domain wall energy obtained by discretizing the gradient of the polarization in **Eq.1**, where w is the domain wall width shown in **Fig.2**. We then integrate $u_{W,i}$ over the domain wall region delimited by the red line in **Fig.2** and along t_{Fe}, and then normalize to d^2, and thus obtain U_W in **Eq.4**.

The difference between the MFM, MFIM and MFMIM systems is in the U_{ET} defined in **Eq.3**. In a MFM the last term in **Eq.3** is zero and $E_{F,T}=V_T/t_F$, so that $U_{ET}=-V_T\sum_{j=1}^{n_D}P_j-(n_D\,C_F\,V_T^2)/2$ with $C_F=\varepsilon_0\varepsilon_F/t_F$. For the MFMIM structure the metal interlayer results in a one dimensional electrostatics, so that $E_{F,T}$ and V_D are independent of $\bar{r}$ and we have $E_{F,T}=(C_DV_T-P_{AV})/(t_FC_0)$, $V_D=(C_FV_T+P_{AV})/C_0$ [7], where $P_{AV}=(\sum_{j=1}^{n_D}P_j)/n_D$ is the average polarization, $C_D=\varepsilon_0\varepsilon_D/t_D$ and $C_0=(C_D+C_F)$. This readily leads to the U_{ET}^{MFMIM} in **Eq.5**, with $C_S^{-1}=C_F^{-1}+C_D^{-1}$. For the MFIM system the electrostatics is three dimensional and the Appendix sketches a derivation of U_{ET}^{MFIM} in **Eq.5**, where capacitances $C_{i,j}$ obey the sum rule $\sum_{i,j=1}^{n_D}(1/C_{i,j})=n_D/C_0$. In this work the $C_{i,j}$ were evaluated numerically for each MFIM, and then used in all analyses.

The overall free energy can be finally written as $U_T=\sum_{j=1}^{n_D}\left(\alpha P_j^2+\beta P_j^4+\gamma P_j^6\right)+U_W+U_{ET}$, with U_{ET} and U_W given by **Eqs. 4, 5**, and the LG equations are readily given by **Eqs.6,7,8**, where **Eq.6** implicitly defines ∂U_{LG}. When t_D tends to zero, $1/C_0$ and $1/C_{j,h}$ also tend to zero while $[C_D/C_0]$ tends to one, so that **Eqs.7,8** simplify to **Eq.6**. For $n_D=1$ **Eqs.7,8** are identical and the MFMIM and MFIM systems are equivalent, furthermore the U_W in **Eq.4** is zero and **Eqs.7,8** simplify to the single domain equation [7].

IV. Conditions for a stable NC operation

The stable NC operation can be evaluated by inspecting the three Jacobian matrices, **J**, of **Eqs. 6, 7, 8** evaluated for P_i=0 in all domains[1], which have the expressions in **Eq.9**, where **I** is the identity matrix while **L** is the Laplacian matrix[2]. Moreover, the matrix $\mathbf{O}_{dep}$ is the all-ones matrix, whereas the entries of $\mathbf{C}_{dep}$ are defined as $\mathbf{C}_{dep}(i,j)=\left[C_{i,j}^{-1}+C_{j,i}^{-1}\right]/2$.

[1]The Jacobian matrix of the system of dynamic equations $dP_i/dt=f_i(P_1,\cdots P_{nD})$ is defined component-wise as $J(i,j)=\partial f_i/\partial P_j$.

[2]**L** is defined component-wise as $\mathbf{L}(i,j)=-1$ if domain j is a neighbour of domain i and $\mathbf{L}(i,j)=0$ otherwise (see **Fig.1**), and $\mathbf{L}(i,i)=-\sum_{j\neq i}\mathbf{L}(i,j)$.

The matrices $\mathbf{O}_{dep}$ and $\mathbf{C}_{dep}$ denote the remarkably different contributions of the depolarization energy to the Jacobian of respectively the MFMIM and MFIM system. The eigenvalues of the symmetric **J** matrices are real valued and the stability for all P_i=0 requires that the largest eigenvalue $\sigma_{max}(\mathbf{J})$ be negative [10], resulting in the inequalities of **Eqs.10**, where σ_{min} denotes the smallest eigenvalue of a matrix.

MFM system. The eigenvalues of **L** are known analytically and the smallest and second smallest eigenvalue are $\sigma_0(\mathbf{L})$=0 and $\sigma_1(\mathbf{L})$=$[2\sin(\pi/(2\sqrt{n_D}))]^2$ [11]. Hence, as expected, in virtue of **Eq.10** the MFM cannot have a stable NC operation.

MFMIM system. Due to the specific form of $\mathbf{O}_{dep}$, analytical eigenvalues for $[(t_F\,k)/(d\,w)\mathbf{L}+\mathbf{C}_{dep}]$ can be derived (*not shown*), and the stability condition is given by **Eq.11**. Hence the effect of $\mathbf{O}_{dep}$ on stabilization is very limited, in fact, compared to MFM, $\mathbf{O}_{dep}$ can only eliminate the influence of $\sigma_0(\mathbf{L})$=0 but not the influence of $\sigma_1(\mathbf{L})$. **Eq.11** also affirms that $(1/C_0)>2|\alpha|t_F$ is necessary for NC stabilization of MFMIM, but not at all sufficient. In particular, for a relatively large n_D such that $\sin(\pi/(2\sqrt{n_D}))\simeq\pi/(2\sqrt{n_D})$, **Eq.11** shows that the k/w necessary for stability increases proportionally to n_D.

MFIM system. For the MFIM structure it is not possible to derive analytical eigenvalues and stability conditions from **Eq.10**, but a numerical analysis shows that $\mathbf{C}_{dep}$ has a much larger influence on NC stabilization than $\mathbf{O}_{dep}$ has for the MFMIM system. It can be demonstrated (*not shown*) that $(1/C_0)>2|\alpha|t_F$ still is a necessary condition for stability.

All results of this work were obtained for ε_F=33, ε_D=23.5, t_F=11.6 nm, t_D=13.5 nm, α=$-4.6{\cdot}10^8$ m/F and β=$9.8{\cdot}10^9$ m^5/C^2/F (i.e. the parameters in [2]), if not otherwise stated.

Fig.3 reports the maximum eigenvalue σ_{max} of the Jacobian versus the coupling factor k for either MFMIM or MFIM structures with an area A=2500nm^2, and for different n_D and d. MFIM achieves NC stabilization for smaller k values compared to the MFMIM and has a much weaker sensitivity to the increase of n_D. By evaluating σ_{max} of the Jacobian as in **Fig.3**, the design space for a stable NC operation can be explored for different material and design parameters.

V. Results and insight about a stable NC operation

The huge difference in the NC stabilization of MFMIM and MFIM systems for large n_D is illustrated in **Fig.4**, showing that for the MFMIM system the k value required for NC stabilization increases proportionally to n_D and thus the device areas. This makes NC stabilization practically impossible for MFMIM systems having areas as those used in recent experiments [2]–[5]. **Fig.5** reports design regions for a stable NC operation of a MFIM structure in the t_D, k plane and for n_D=100. The NC operation is not possible for too thin oxides because of the necessary condition $(1/C_0)>2|\alpha|\,t_F$. Moreover, for any t_D there exists a minimum k value for NC stabilization, that becomes independent of t_D for t_D larger than about 10 nm. This occurs because the electric field lines tend to close inside the oxide and the depolarization energy becomes independent of t_D (*not shown*). The MFIM results in **Fig.5** are insensitive to an increase of n_D, whereas for a MFMIM the k for stability increases proportionally to n_D (see **Fig.3**), which precludes stability for the k values in **Fig.5**. **Fig.5** also shows that the empirical formula for MFIM stability in [7] gives k values in fair agreement with our results.

Eqs.9-11 and **Fig.5** describe NC stabilization in the condition P_i=0 for all domains. We also solved numerically **Eqs.7-8** to inspect the steady-state domain configuration corresponding to V_T=0, which is illustrated in **Fig.6** for a MFIM and a MFMIM system with k=$2\cdot10^{-9}$ m^3/F and n_D=100. Consistently with **Fig.5**, the steady-state condition for the MFIM system corresponds to all P_i=0. The MFMIM, instead, is not stable for all P_i=0, and therefore it evolves to a configuration corresponding to P_{AV}=$(\sum_{i=1}^{n_D}P_i)/n_D\simeq$0.

The crucial difference between MFMIM and MFIM systems is that the depolarization energy of the MFMIM system at V_T=0 is zero if P_{AV} is zero (see **Eq.5**). Consequently, if the MFMIM is initialized with all P_i=0, then it gets destabilized along trajectories having $P_{AV}\simeq$0 and thus $U_{ET}^{MFMIM}\simeq$0, which is confirmed by the steady-state configuration in **Fig.6(b)**. The same trajectories are not possible for the MFIM system because the corresponding U_{ET}^{MFIM} in **Eq.5** is not at all zero, hence it is the form of the U_{ET}^{MFIM} which makes the NC stabilization of the MFIM system possible.

VI. Comparison with experiments

In order to validate our models and the NC stabilization analysis in Sec.V, we now illustrate a comparison with experiments for the MFIM capacitor in [1], [2]. Simulations correspond to n_D=100 and d^2=25nm^2, and we verified that results are practically insensitive to a further n_D increase. We used a deliberately small ρ value to make the ferroelectric time constants negligible, k=$2{\cdot}10^{-9}$ m^3/F (i.e. stable NC operation, see **Figs.5, 6**), and included a fixed charge Q_{DF}=$-0.15C/m^2$ at the ferroelectric-insulator interface [1]. **Fig.7(a),(c)** report the charge Q=$P+\varepsilon_F\varepsilon_0E_F$ and field E_F versus the V_{MAX} of the trapezoidal external waveform, and **Fig.7(b)** shows P versus E_F. The agreement between simulations and measurements is good for all the main features of the experiments.

We also developed a model for traps at the ferroelectric-dielectric interface (see **Fig.8**), with a first order kinetic given by $\partial n_t/\partial t$=$c_n(N_T-n_t)-e_nn_t$, with n_t, N_T being trapped electron and trap density. The relation c_n=$e_n\exp[(E_{fB}-E_{Tr})/KT]$ ensures that the static trap occupation is in equilibrium with $E_{f,B}$. **Fig.9** shows that by increasing N_T the MFIM tends to deviate from the stable NC region, in which case the MFIM trajectories become sensitive to the input frequency (see **Fig.10**), which is again in qualitative agreement with [2].

VII. Conclusions

We have presented comprehensive revised analysis of stable NC operation in ferroelectric capacitors, reported analytical and numerical results and explained why in MFMIM systems instability seems inevitable. We also show that traps can play a subtle role in MFIM systems. Good agreement with experiments validate our modelling approach and our conclusions.

Free energy, $\bar{r}=(x,y)$	Ferroelectric (spontaneous and dielectric): $u_F = \alpha P^2 + \beta P^4 + \gamma P^6 + k\,(\nabla P)^2 + \frac{\varepsilon_0 \varepsilon_F}{2} E_F^2$ [J/m^3]	(1)
D_i: area of domain i	$\mathcal{U}_F = \frac{V_T}{2}\int_A \varepsilon_0\varepsilon_F E_{F,T}(\bar{r})d\bar{r}$, $\mathcal{U}_B = -V_T\left[d^2\sum_{j=1}^{n_D} P_j + \int_A \varepsilon_0\varepsilon_F E_{F,T}(\bar{r})d\bar{r}\right]$, $\mathcal{U}_D = \sum_{j=1}^{n_D}\int_{D_j}\frac{P_j V_D(\bar{r})}{2}d\bar{r}$ [J]	(2)
	$U_{ET} = -\frac{V_T}{2}\frac{1}{d^2}\int_A \varepsilon_0\varepsilon_F E_{F,T}(\bar{r})\,d\bar{r} - V_T\sum_{j=1}^{n_D} P_j + \frac{1}{d^2}\sum_{j=1}^{n_D}\int_{D_j}\frac{P_i\,V_D(\bar{r})}{2}\,d\bar{r}$ [J/m^2]	(3)
	Domain i: $u_{W,i} = k\sum_n[(P_i - P_n)/w]^2$ [J/m^3] Overall domain wall: $U_W = \sum_{i=1}^{n_D}\left[\frac{t_F}{2d}\sum_n \frac{k}{w}(P_i - P_n)^2\right]$ [J/m^2]	(4)
Electrost. energy	$U_{ET}^{MFMIM} = \frac{n_D P_{AV}(P_{AV} - V_T C_D)}{2C_0} - \frac{C_S V_T^2}{2} n_D$, $U_{ET}^{MFIM} = \frac{1}{2}\sum_{i,j=1}^{n_D}\frac{P_i P_j}{C_{i,j}} - V_T\frac{C_D}{C_0}\sum_j^{n_D} P_j - \frac{C_S V_T^2}{2} n_D$	(5)
Dynamic	MFM: $t_F\rho\frac{dP_i}{dt} = \frac{\partial U_T}{\partial P_i} = -t_F\left(2\alpha P_i + 4\beta P_i^3 + 6\gamma P_i^5\right) - \frac{t_F k}{dw}\sum_n (P_i - P_n) + V_T = \partial U_{LG} + V_T$	(6)
Landau-Ginzburg	MFMIM: $t_F\,\rho\frac{dP_i}{dt} = \partial U_{LG} - \frac{1}{n_D C_0}\sum_{i=1}^{n_D} P_i + \frac{C_D}{C_0}V_T$	(7)
equations	MFIM: $t_F\rho\frac{dP_i}{dt} = \partial U_{LG} - \frac{1}{2}\sum_{j=1}^{n_D}\left[\frac{1}{C_{i,j}} + \frac{1}{C_{j,i}}\right]P_j + \frac{C_D}{C_0}V_T$	(8)
Jacobian matrices	$\mathbf{J}_{MFM} = \frac{1}{\rho t_F}\left[-2\alpha t_F\mathbf{I} - \frac{t_F k}{dw}\mathbf{L}\right]$, $\mathbf{J}_{MFMIM} = \mathbf{J}_{MFM} - \frac{1}{\rho t_F}\left[\frac{\mathbf{O}_{dep}}{n_D C_0}\right]$, $\mathbf{J}_{MFIM} = \mathbf{J}_{MFM} - \left[\frac{\mathbf{C}_{dep}}{\rho t_F}\right]$	(9)
Condition for stable	MFM: $\frac{k}{dw}\sigma_{min}(\mathbf{L}) > 2\lvert\alpha\rvert$, MFMIM: $\sigma_{min}\left[\frac{t_F k}{dw}\mathbf{L} + \frac{\mathbf{O}_{dep}}{n_D C_0}\right] > 2\lvert\alpha\rvert t_F$, MFIM: $\sigma_{min}\left[\frac{t_F k}{dw}\mathbf{L} + \mathbf{C}_{dep}\right] > 2\lvert\alpha\rvert t_F$	(10)
NC operation	Analytic condition for MFMIM: $\sigma_{min}\left[\frac{t_F k}{dw}\mathbf{L} + \frac{\mathbf{O}_{dep}}{n_D C_0}\right] = \min\left\{\frac{1}{C_0}, \frac{t_F k}{dw}\left[2\sin\left(\pi/(2\sqrt{n_D})\right)\right]^2\right\} > 2\lvert\alpha\rvert t_F$	(11)
Appendix.	V_T and P_i are the electric field sources and linearity allows us to write $E_{F,T}(\bar{r}) = \sum_{j=1}^{n_D} P_i G_{FT,j}(\bar{r}) + (C_D V_T)/(t_F C_0)$, $V_D(\bar{r}) = \sum_{j=1}^{n_D} P_i G_{D,j}(\bar{r}) + (C_F V_T)/C_0$, where $G_{(FT,D),j}$ are Green's functions of P_i. By substituting $E_{F,T}$, $V_D(\bar{r})$ in **Eq.3** it is possible to derive U_{ET}^{MFIM} in **Eq.5**, with no approximations and by defining $[C_{i,j}]^{-1} = d^{-2}\int_{D_i} G_{D,j}(\bar{r})d\bar{r}$.	

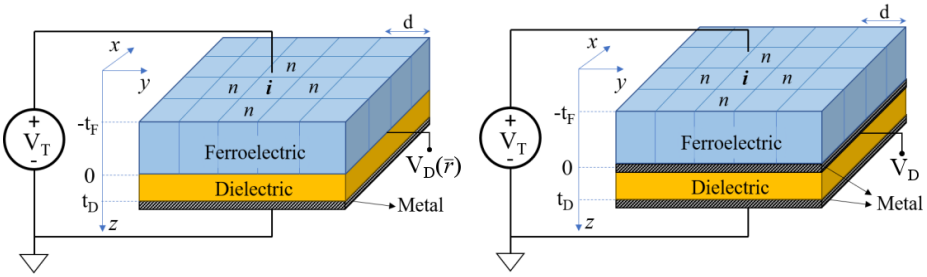

Fig. 1: Sketch of a MFIM (left) and a MFMIM capacitor (right), where the top metal contact is not shown. t_F and t_D are the ferroelectric and dielectric thicknesses, d is the side of a square domain with area d^2, and V_T is the externally applied voltage. $V_D(\bar{r})$ is the electrostatic potential at the oxide interface (i.e. at z=0), which depends on $\bar{r}$ in a MFIM but it is independent of $\bar{r}$ in a MFMIM capacitor.

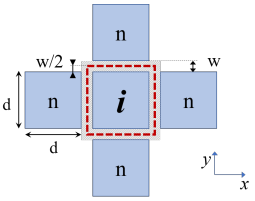

Fig. 2: Sketch of domain i and its nearest neighbor domains n. The shaded area illustrates the domain-wall region, whose width is w. The dashed red line delimits the domain-wall region used to calculate $u_{W,i}$ in **Eq.4**.

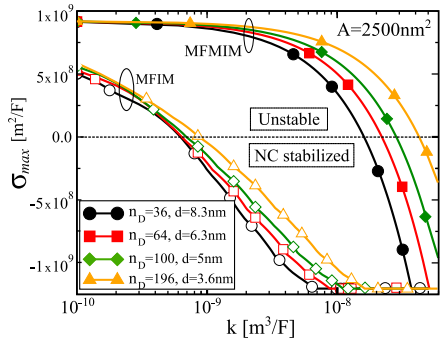

Fig. 3: Largest eigenvalue σ_{max} of the Jacobian matrix for all P_i=0 versus the domain wall coupling factor k for either a MFIM (numerically calculated) or a MFMIM structure (see **Eq.11**). Capacitor area is A=2500nm^2 and results are shown for different combinations of d and n_D. Stable NC operation corresponds to σ_{max}<0.

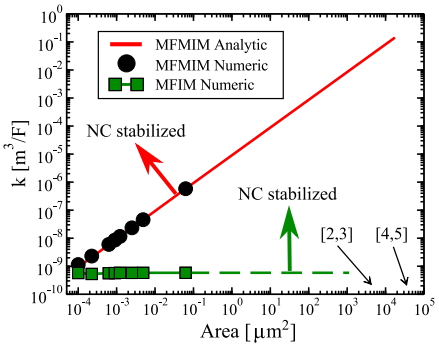

Fig. 4: Minimum coupling factor k necessary for a stable NC operation versus the capacitor area for either a MFMIM or a MFIM structure. For the MFIM structure results have been calculated numerically from the condition σ_{max} <0, while for the MFMIM structure results stem from **Eq.11**. Domain size is d=5nm, thus Area=d^2 n_D. Please notice the large areas corresponding to recent experiments in [2]–[5].

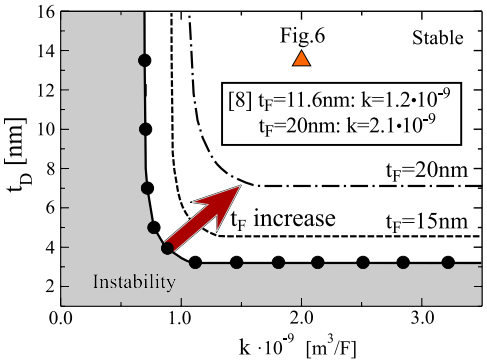

Fig. 5: Regions for stable NC operation for a MFIM structure in the t_D versus k plane and for different t_F values. Filled circles correspond to t_F=11.6nm. For larger t_F values the minimum t_D required for stability increases as predicted by the necessary condition $(1/C_0)>2|\alpha|\,t_F$. Area A=2500nm^2 and n_D=100.

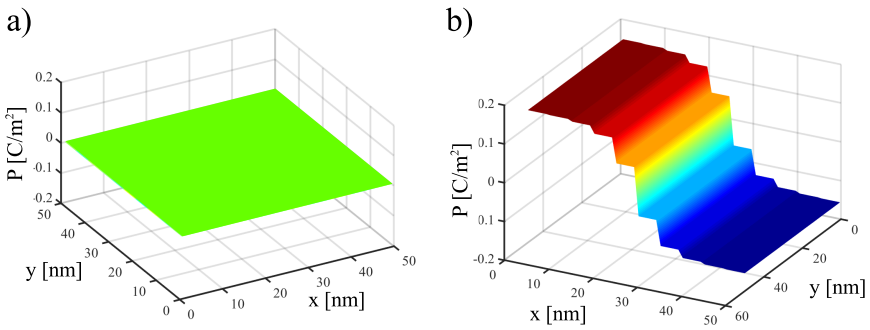

Fig. 6: Steady-state domain configuration at V_T=0V for either a MFIM (a) or a MFMIM capacitor (b). Both structures have k=2·10^{-9}, t_D=13.5nm and t_F=11.6nm, that for the MFIM system correspond to a stable NC operation (see the triangular symbol in **Fig.5**), but it is instead unstable for the MFMIM case (*not shown*).

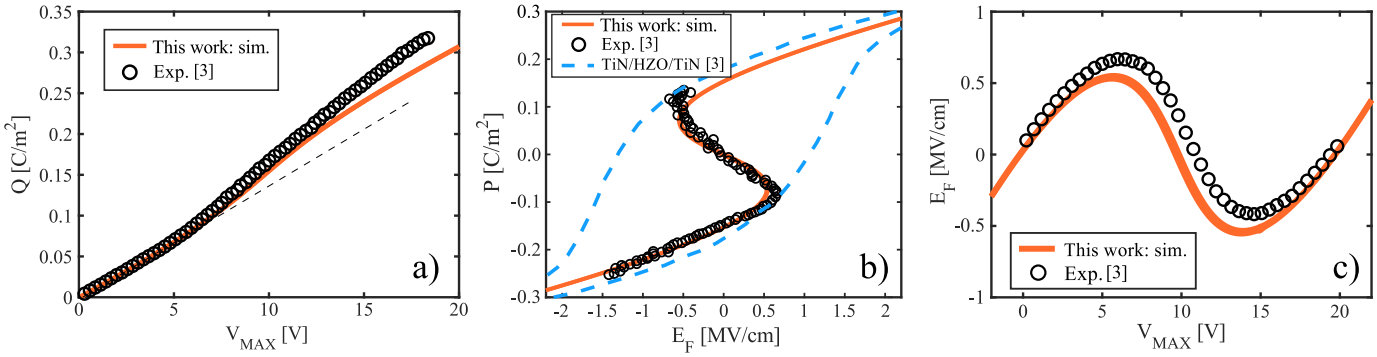

Fig. 7: Measurements (symbols) and simulations (red lines) for the MFIM structure in [1], [2], consisting of a ferroelectric $Hf_{0.5}Zr_{0.5}O_2$ layer and a Ta_2O_5 insulator. (a) Reversibly stored and released charge, Q, versus the top value V_{MAX} of the trapezoidal voltage waveform across the capacitor. (b) Polarization versus ferroelectric electric field. (c) Ferroelectric electric field versus V_{MAX}. Simulation parameters are ε_F=33, ε_D=23.48, t_F=11.6nm, t_D=13.5nm, $\alpha=-4.6\cdot10^8$m/F, $\beta=9.8\cdot10^9$m^5/C^2/F, ρ=0.5 mΩ·m and $k=2\cdot10^{-9}$ m^3/F.

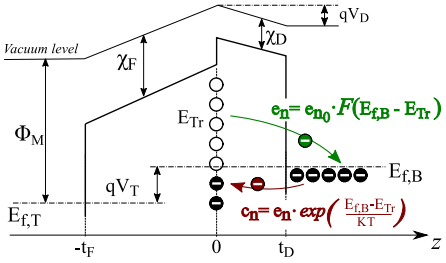

Fig. 8: Band profile for the MFIM structure in the presence of traps at the ferroelectric-oxide interface. $E_{f,B}$ and $E_{f,T}$ are Fermi levels of bottom and top metal contacts and E_{Tr} is the trap energy. Traps exchange electrons with bottom metal contact via tunneling with emission, e_n, and capture rate, c_n, where $F_0(\eta)$ is the Fermi occupation function. Other symbols have their standard meaning and values Φ_M=4.05eV, χ_F=2.2eV, χ_D=0.9eV and e_{n0}=5.6·10^7 1/s.

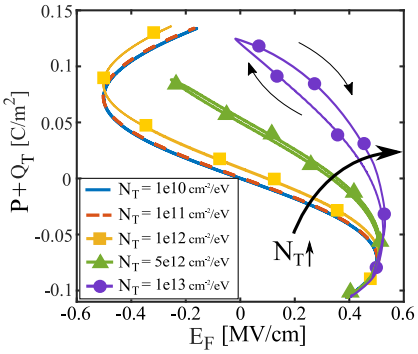

Fig. 9: Charge versus ferroelectric E_F for the MFIM in [2] and for different densities, N_T, of interface traps (see **Fig.8**) with uniform distribution. To ensure that all traps are responding, frequency is set to 1KHz. Arrows show clockwise hysteresis due to traps.

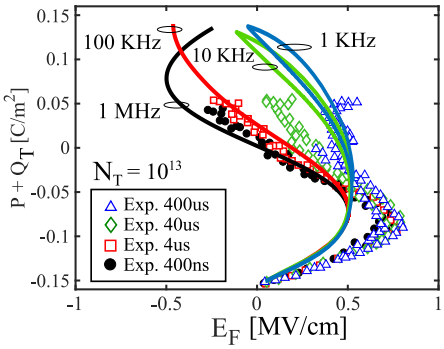

Fig. 10: Charge versus ferroelectric E_F for the MFIM in [2], with uniform trap density N_T=10^{13} eV^{-1}/cm^2 and for different frequencies of the input V_T waveform. Symbols are experiments [2] and lines are simulations.

References

[1] M. Hoffmann *et al.*, *IEDM*, pp.31.6.1-31.6.4, 2018
[2] M. Hoffmann *et al.*, *Nature*, vol.565, pp.464-467, 2019
[3] Z. Liu *et al.*, *IEDM*, pp.31.2.131.2.4, 2018
[4] X. Li *et al.*, *IEDM*, pp.31.3.131.3.4, 2018
[5] H. Wang *et al.*, *IEDM*, pp.31.3.131.3.4, 2018
[6] J. Van Houdt *et al.*, *EDL*, vol. 39, n. 6, pp.877-880, 2018
[7] M. Hoffmann *et al.*, *Nanoscale*, vol. 10, pp.891-899, 2018
[8] M.A. Alam *et al.*, *App. Phys. Lett.*, vol. 114, n. 9, 2019
[9] M. Purcell *et al.*, *Electricity and Magnetism*, Cambridge Univ. Press, 2013
[10] D.G. Luenberger, *Intro. to Dynamic Systems*, John Wiley & S., 1979.
[11] M. Fielder, *Czechoslovak Mathematical J.*, vol.23, pp.298-305, 1973